A NEW MARINE PRASINOPHYTE GENUS ALTERNATES BETWEEN A FLAGELLATE AND A DOMINANT BENTHIC STAGE WITH MICRORHIZOIDS FOR ADHESION

Richard Wetherbee[2]*,*
School of BioSciences, University of Melbourne, Victoria 3010, Australia

Vanessa R. Marcelino,
Westmead Institute for Medical Research, The University of Sydney, Westmead, New South Wales 2145, Australia

Joana F. Costa, Brenna Grant, Simon Crawford,
School of BioSciences, University of Melbourne, Victoria 3010, Australia

Ross F. Waller,
Department of Biochemistry, University of Cambridge, Cambridge, UK

Robert A. Andersen,
Friday Harbor Laboratories, University of Washington, Seattle, USA

Drew Berry,
The Walter and Eliza Hall Institute of Medical Research, Parkville, Victoria 3052, Australia

Geoffrey I. McFadden and Heroen Verbruggen[2]
School of BioSciences, University of Melbourne, Victoria 3010, Australia

[2]Authors for correspondence: richardw@unimelb.edu.au, heroen@unimelb.edu.au

Abstract:

Prasinophytes (Chlorophyta) are a diverse, paraphyletic group of planktonic microalgae for which benthic species are largely unknown. Here, we report a sand-dwelling, marine prasinophyte with several novel features observed in clonal cultures established from numerous locations around Australia. The new genus and species, which we name *Microrhizoidea pickettheapsiorum* (Mamiellophyceae), alternates between a benthic palmelloid colony, where cell division occurs, and a planktonic flagellate. Flagellates are short lived, settle and quickly resorb their flagella, the basal bodies then nucleate novel tubular appendages, termed "microrhizoids", that lack an axoneme and function to anchor benthic cells to the substratum. To our knowledge, microrhizoids have not been observed in any other green alga or protist, are slightly smaller in diameter than flagella, generally contain 9 microtubules, are long (3-5 times the length of flagella) and are not encased in scales. Following settlement, cell divisions result in a loose, palmelloid colony, each cell connected to the substratum by two microrhizoids. Flagellates are round to bean-shaped with two long, slightly uneven flagella. Both benthic cells and flagellates, along with their flagella, are encased in thin scales. Phylogenies based on the complete chloroplast genome of *Microrhizoidea* show it is clearly a member of the Mamiellophyceae, most closely related to *Dolichomastix tenuilepsis*. More taxon-rich phylogenetic analyses of the 18S rRNA gene, including metabarcodes from the Tara Oceans and Ocean Sampling Day projects, confidently show the distinctive nature of *Microrhizoidea,* and that the described biodiversity of the Mamiellophyceae is a fraction of its real biodiversity. The discovery of a largely benthic prasinophyte changes our perspective on this group of algae and, along with the observation of other potential benthic lineages in environmental sequences, illustrates that benthic habitats can be a rich ground for algal biodiscovery.

Key index words: Chlorophyta; basal bodies; Dolichomastigales; environmental sequences; Mamiellophyceae; *Microrhizoidea*; microrhizoids; molecular phylogeny; sand-dwelling

Abbreviations: df, distal fiber; ML, maximum likelihood; MTOC, microtubule organizing center; OTU, operational taxonomic unit; pf, proximal fiber; R1, microtubule root #1; R2, microtubule root #2; R3, microtubule root #3; SR, striated root; tr, transition region

INTRODUCTION

Prasinophytes are a paraphyletic group of planktonic, green microalgae in the Chlorophyta. Historically, our knowledge of the prasinophytes comes from studies of a small selection of species isolated from surface plankton tows, some available from culture collections, while other habitats were largely unexplored. During the last decade, environmental cataloguing using 18S sequencing has revealed an extensive, worldwide distribution of the prasinophyte class Mamiellophyceae, including both pico-sized and nano-sized cells in a wide range of habitats, from the Arctic to tropical waters (e.g., Vaulot et al. 2008, Not 2008, Monier et al. 2013, 2015). The contribution of the fast-growing, picoplanktonic representatives to oceanic biomass has become evident (Worden et al. 2004), and evidence suggests these populations are easily impacted by environmental disturbances such as those brought on by climate change.

Monitoring the diversity and distribution of Mamiellophyceae populations has become an important endeavour in attempting to understand their importance to global primary production. Prasinophytes are typically thought of as marine planktonic algae, and environmental sequencing confirms there is a large biodiversity of species in those types of habitats (e.g. Monier et al. 2016). Interestingly, environmental sequences also suggest that Mamiellophyceae may exist in some benthic habitats (Marin and Melkonian 2010, Monier et al. 2015, 2016). In other prasinophyte classes, reports of benthic representatives have been rare, for example the sand-dwelling *Pyramimonas octopus* Moestrup & Kristiansen in the Pyramimonadophyceae (Moestrup et al. 1987), but to date no benthic Mamiellophyceae have been described.

Following the description of the Mamiellales as an order by Moestrup (1984), this group was elevated to the class level by Marin & Melkonian (2010). The group includes non-flagellate and biflagellate unicells with a relatively simple scale covering, where scales of similar ultrastructure and dimensions were found on both the cell and flagella (though some species lack scales). Two orders were distinguished within the class, the Monomastigales and Dolichomastigales, the latter containing the new family Dolichomastigaceae with a single genus *Dolichomastix* (Marin & Melkonian 2010). Also included was an unusual clade (Dolicho_B) comprised of environmental rDNA sequences from deep sea sediments (Marin & Melkonian 2010).

During our exploration of sand-dwelling microalgae, we discovered a new benthic Mamiellophyceae species. The goal of this study is to describe this species, which we name *Microrhizoidea pickettheapsiorum*, investigate its adaptations to life in a benthic habitat, and infer its phylogenetic position among the prasinophytes. Our approach consists of light and electron-microscopic observations of culture strains, and phylogenetic inference based on whole chloroplast genomes as well as 18S rDNA sequences from cultured strains and environmental sequencing projects.

MATERIALS AND METHODS

Sampling, isolation and culture. A first sand sample was collected in a high intertidal rock pool from Trial Bay, Tasmania, approximately 20 m East of the Jetty (43° 07' 54"S; 147° 15' 19"E) in January, 2009. The sample consisted of approximately 0.5 - 1.0 cm of sand plus seawater that was placed into a 60 ml plastic jar and returned to the lab. A clonal culture (TasT39) was established by isolating the flagellate stage of the species under investigation from a field sample by micro-pipetting into K-enriched seawater medium (Keller *et al.* 1987). The culture was maintained in 60 ml plastic containers at 21^{o}C under Sylvania 58 Luxline Plus and Gro-Lux fluorescent lamps with a daily 10:14 hr light:dark cycle; a stock culture was transferred into new K-medium once a month. Additional strains were collected, isolated and cultured from Five Finger Bay (strain 5FNG), West Australia (23° 10' 39"S; 113° 45' 48"E), Noah's Beach (NB3), tropical north Queensland (16° 08' 03"S; 145° 27' 07"E) and Wye River (Wye4), Victoria (38° 38' 20"S; 143° 53' 34"E). For comparison, a culture of *Dolichomastix tenuilepsis* was obtained (strain K-0587, NIVA Culture Collection of Algae, from the SCCPA in Copenhagen prior to its closure) and maintained as above for *M. pickettheapsiorum*.

Light and electron microscopy. To observe the flagellate stage, a drop of cell culture was taken 4 hours after the beginning of the light period when flagellates were prevalent, and mounted onto microscope slides with coverslips sealed with a 1:1:1 ratio of Vaseline, lanoline, and paraffin wax. For benthic cells and microrhizoids, 5 ml of culture containing flagellates was poured over coverslips in small petri dishes and allowed to settle and grow for 3-5 days. Coverslips were then removed and inverted onto microscope slides and mounted as above. Living flagellates and benthic cells were observed and recorded using a Zeiss AxioPlan 2 microscope (Carl Zeiss, Oberkochen, Germany) and photographs were taken using a Canon EOS 60D digital single-lens reflex camera (Canon USA, Melville, New York, USA).

To prepare whole mounts of *M. pickettheapsiorum* flagellates, 50 ml of log phase cultured cells where flagellates were plentiful were centrifuged at low speed to a pellet using a handheld centrifuge. Cells were resuspended in 1 ml of fresh K-medium, and a single drop of cell suspension was placed on a coated copper grid. The grid was then placed next to a drop of osmium tetroxide (4%) under an inverted Petri dish and the vapors allowed to fix the cells for 5 min. The grids were then washed three times with distilled water and allowed to dry. A drop of 2% uranyl acetate in distilled water was then placed on the grid for 2 min, and then extracted from the side of the grid using filter paper. Grids were allowed to dry overnight and subsequently imaged using a Tecnai Spirit transmission electron microscope (FEI) equipped with an Eagle 2K CCD camera

For transmission electron microscopy, the flagellate stage was most plentiful approximately 4 hours into the light period, and was concentrated by gentle centrifugation to obtain a cell slurry of 5 ml ready to fix. For benthic cells and their delicate microrhizoids, another preparation was necessary. A hot, 2% agarose

solution (1 ml) was poured into small, 20ml petri dishes producing a thin coating that was allowed to set and act as a soft yet firm substratum. Approximately 5 ml of culture media with flagellates were added to the petri dish and flagellates were allowed to settle on the agarose film. Benthic cells divided and microrhizoids became plentiful after 3-5 days. Cells were chemically fixed using the following recipe; 2.5 ml of a 4% solution of glutaraldehyde mixed with 2.5 ml of a 4% solution of osmium tetroxide, both in K-seawater media on ice (a total of 5 ml). The fixative was mixed with 5 ml of the cell slurry, or added to the petri dishes that contained the benthic cells in 5 ml of media, and left for one hour before being washed 3x with K-media. Cells were then brought into distilled water in steps: 75:25, 50:50 and 25:70 K-media:distilled water. Cells were washed 3 times in distilled water and placed in a solution of 2% uranyl acetate in distilled water for one hour before gradual dehydration in EtOH (10%, 25%, 50%, 75%, 90% and 3x at 100%). Cells were then gradually embedded in either LR White (Merck) or Spurr's medium (Spurr, 1969). Thin (70 nm) sections were cut from either pellets of the flagellate preparation, or from plugs cut from the agarose films, using a Leica Ultracut S ultramicrotome and post-stained with 1% aqueous uranyl acetate and triple lead stain (Hanaichi et al., 1986). The sections were imaged using a Tecnai Spirit transmission electron microscope (FEI) equipped with an Eagle 2K CCD camera.

Molecular work. Total genomic DNA was extracted using a modified CTAB protocol (Cremen et al. 2016). The 18S rRNA gene was amplified and sequenced as described in Wetherbee & Verbruggen (2016) and the sequences submitted to Genbank (MN056945-8). To obtain data for chloroplast genome assembly, paired-end libraries were constructed and sequenced with Illumina technology following methods described by Cremen et al. (2018, 2019). For strain T39, we used the HiSeq 2500 platform (paired-end, 125 reads, ~3 Gb of data) and for 5FNG, we used the NextSeq 500 platform (paired-end, 150 bp reads, ~1.5 Gb of data).

Chloroplast genome phylogeny. Assembly of the Illumina reads followed previously published protocols (Marcelino et al. 2016, Jackson et al. 2018) and the resulting contig was annotated using MFannot for rRNAs and CDSs and ARAGORN for tRNAs (Laslett & Canback 2004, Beck & Lang 2010) and submitted to Genbank (MN056173).

Chloroplast genomes for other green algae were obtained from Genbank. Most of the taxon sampling is in prasinophytes, but we also added a selection of representative "core chlorophyta" (Fučíková et al. 2014) and included two streptophytes as outgroups. Since no chloroplast genomes have been published for the Mamiellophyceae *Dolichomastix* and *Crustomastix*, we sourced chloroplast-encoded genes for these species from the MMETSP project (Keeling et al. 2014), limiting ourselves to the longest genes. This process involved extracting named genes >800 bp from the *Ostreococcus tauri* chloroplast genome and using them as queries for BLAST searches against the re-assembled MMETSP

transcriptomes (Johnson et al. 2018). This identified 8 genes for *Crustomastix* (*atp*A, *atp*B, *psb*A, *psb*B, *psb*C, *psb*D, *rbc*L, *rpl*2) and 11 in *Dolichomastix* (*atp*A, *atp*B, *pet*A, *psa*A, *psa*B, *psb*A, *psb*B, *psb*C, *psb*D, *rbc*L, *tuf*A).

All named protein-coding genes except those with fewer than 10 taxa and the poorly conserved *rpo*A/B/C and ftsH were aligned based on their corresponding amino-acids with TranslatorX v.1.1 (Abascal et al. 2010), using Muscle v3.8.31 as the alignment algorithm (Edgar 2004). Following a visual check of the 69 retained alignments, they were concatenated and the resulting supermatrix analysed with maximum likelihood (ML) analysis in RAxML v.8.2.12 (Stamatakis 2014) using the CPREV+CAT+F model and 100 rapid bootstraps. The same analysis was repeated after GBlocks was applied (Talavera & Castresana 2007).

18S rRNA phylogenies. In order to infer more taxon-dense phylogenies and attempt to identify potential close relatives of *M. pickettheapsiorum*, we performed phylogenetic analysis of the 18S rRNA gene using data available from Genbank and environmental sequencing projects. Three datasets were assembled.

The first alignment contained only relatively long sequences (>600 nt) downloaded from Genbank. Sequences were retrieved with a blastn search against Genbank using the *M. pickettheapsiorum* 18S sequence as a query using default settings in Geneious (Kearse et al. 2012), and we downloaded all sequences of Dolichomastigaceae used in Marin and Melkonian (2010) as well as a representative set of more distantly related prasinophytes. An initial alignment was produced in Geneious with MAFFT Auto (Katoh et al. 2013). To filter the initial dataset down to a more convenient size, a UPGMA tree (Tamura-Nei distance model) was constructed, and based on this tree 1-2 sequences from the non-focal prasinophyte clades I and III – VII were chosen and the remainder removed. The final alignment was inferred with MAFFT L-INS-i. The best-fitting substitution model (TIM3e+R3) was selected with the Bayesian Information Criterion using ModelFinder implemented in IQ-Tree v.1.6.2 (Nguyen et al., 2015; Kalyaanamoorthy et al., 2017). A maximum likelihood tree was reconstructed with IQ-Tree using 100,000 ultrafast bootstrap replicates (Hoang et al. 2018).

The second and third datasets used the large environmental datasets available from the Ocean Sampling Day (OSD) and Tara Oceans expedition, respectively, in order to place *M. pickettheapsiorum* in the context of the larger diversity of Mamiellophyceae observed in these global environmental surveys using culture-independent high-throughput sequencing, Operational Taxonomic Units (OTUs) sequences from OSD classified as Dolichomastigaceae (Tragin and Vaulot 2018), and OTUs from Tara Oceans (Bork et al. 2015) classified as Mamiellales or Dolichomastigales (Monier et al. 2016) were used to

produce phylogenies. OSD and Tara Oceans used different regions of the 18S rRNA, and therefore they were analysed separately. The alignments and phylogenetic tree reconstructions were performed as above. The 18S rRNA alignments are available from FigShare (https://doi.org/10.6084/m9.figshare.8251541.v1).

RESULTS

Chloroplast genome phylogeny. The chloroplast genome of *M. pickettheapsiorum* is a circular-mapping molecule of 92,720 base pairs without inverted repeat and it contains the chloroplast-encoded genes typically found in other prasinophytes (Fig. S1). The phylogenies derived from the chloroplast genome data clearly show that *M. pickettheapsiorum* is nested in the Mamiellophyceae, as a sister lineage of *Dolichomastix tenuilepis* (Fig. S2). While the phylogeny provides strong support for the association with *Dolichomastix*, the relationships among the main lineages of Mamiellophyceae are not well resolved.

18S rRNA phylogenies. The phylogenies inferred from the 18S rDNA gene show the relationships of *M. pickettheapsiorum* in more taxon-dense datasets including sequences from cultured strains and ribotypes derived from environmental sequencing. The first tree based on relatively long 18S rRNA sequences (Fig. 1) shows *M. pickettheapsiorum* forming a distinctive lineage in the "Dolichomastigaceae A" clade (sensu Marin & Melkonian 2010), although this higher-level clade did not receive statistical support in our analyses. *Microrhizoidea* is the only benthic member of this this clade, which also includes a cultured strain of *Dolichomastix tenuilepis* and several environmental sequences from planktonic samples in the Mediterranean Sea and the USA. The more extensive comparisons with environmental sequences from Tara Oceans and the Ocean Sampling Day (OSD) show similar results, with *M. pickettheapsiorum* forming a distinct lineage without close relatives (Figs S3,S4). The OSD data show a second divergent lineage in the Dolichomastigaceae A lineage, placed just below *M. pickettheapsiorum* in the phylogeny in Fig. S3. This lineage, consisting of five OTUs, was found in planktonic samples from Oslofjord, Iceland, Maine, Italy and the Black Sea. In the Tara Oceans phylogeny (Fig. S4), the apparent closest relatives of *M. pickettheapsiorum* (though statistical support is low) were OTUs 229972 and 68769, which were found mostly in surface waters from the Mediterranean, North Atlantic and Red Sea.

Light microscope observations. Flagellates were rounded to bean shaped, 5.0-6.5 µm in width and 6.0 - 7.5 µm in length including the scale covering (Fig. 2a-c), flattened laterally where the two flagella are inserted (Fig. 2d) at an acute angle to the ventral cell surface. The chloroplast is deeply lobed and appears as two chloroplasts under the light microscope (e.g., Fig. 2c). The chloroplast lobes were observed by transmission electron microscopy to be connected by a narrow isthmus that contained the eyespot (Fig. 2c and see below). Lobes each contained a distinctive pyrenoid with a starch shield (Fig. 2a,b). The two

flagella were between 3.5-5 times the length of the cell (25-35 μm) (Fig. 2a,b) with one flagellum being slightly longer than the other.

Flagellates were short-lived and transformed into benthic cells by attaching to the coverslip surface, flattening out and becoming dome-shaped (5.5-7.5 μm in diameter) (Fig. 2e-i). The two flagella were quickly withdrawn back into the cells (15-20 S) while the scale covering appeared to remain, accumulating at the ends of the retracting flagella (Fig. 2e-h, video at https://youtu.be/Vq-ZgU2nn90) and apparently dispersing into the media, though we could not detect their fate with the light microscope. The chloroplast lobes with enclosed pyrenoids with starch shields were most distinctive in the benthic stage (e.g., Fig. 2i). Following settlement, benthic cells typically enlarged and divided (Fig. 2j,k), the daughter cells each producing two anchoring microrhizoids using the flagella basal bodies as nucleating centers (Fig. 2l-n). Alternatively, some settled cells produced microrhizoids prior to enlarging and dividing.

As benthic cells continued to divide, each cell produced two microrhizoids while secreting an encasing mucilage. Multi-celled, loosely arranged palmelloid colonies developed (Fig. 3a-e). The benthic stage dominated the light:dark cycle, with flagellates appearing 2-4 hours after the lights came on, but were largely unsighted the remainder of the cycle.

Like flagella, microrhizoids of benthic cells were nucleated by the basal bodies, grew out perpendicular to the cell surface, were stiff, never beat, and eventually adhered to the substratum where they continued to grow (Figs. 2l-n, 3a-c,e). Microrhizoids were c. 200nm in diameter and elongated up to 15-18 times the diameter of a cell (i.e., 75 – 110 μm) (Fig. 3a) further anchoring the colony to the substratum (Fig. 2k-m). A two-celled colony produced 4 microrhizoids (i.e., from 4 basal bodies) while the two cells also generated a mucilaginous covering over both cells. The two cells then normally divided to produce a 4-celled colony, producing 4 new microrhizoids for a total of 8, and subsequently divided to form an 8-celled colony with a total of 16 microrhizoids. Larger cell colonies were rare, but it was difficult to locate and follow an increasing number of microrhizoids which dominate the coverslip surface (Fig. 3e).

As colonies increase in size, layers of cells arise above the substratum, thereby requiring microrhizoids to navigate beyond the colony extremity before finding the substratum, often some distance from the colony (Fig. 3b,c). The three-dimensional path of these outlying microrhizoids could be followed in the light microscope, and they almost all locate and intersect the substratum by an unknown mechanism. As benthic colonies grew in size and the mucilage that encased the cells increased in volume, some microrhizoids do not escape the colony proper and deteriorated before reaching the substratum. Colonies larger than 32 cells were not observed in log phase cultures.

During the early part of the light cycle, daughter cells at a colony's interface with the culture media often divided and differentiated into motile cells, growing flagella rather than microrhizoids and escaping the colony (Fig. 3d). Flagella had a prominent scale covering and therefore were much thicker (0.5–0.6 μm) than the thinner, scale-less microrhizoids (c. 0.2 μm). The basal bodies that generate flagella were not orientated perpendicular to the cell surface, as during microrhizoid formation, but at an acute angle to the flagellate surface, and the emerging flagella began to beat almost immediately.

In dense cultures at cell concentrations unlikely to be found in nature, flagellates that did not find a surface for attachment withdrew their flagella (video at https://youtu.be/Vq-ZgU2nn90) and remained planktonic during division, often forming planktonic colonies with microrhizoids that were diminished and never appeared to extend beyond the colonies' mucilage. We never observed motile cells to divide, though it is extremely difficult to prove something is not happening.

For comparison with *M. pickettheapsiorum*, we studied a culture of *D. tenuilepsis* (Throndsen & Zingone 1997, Zingone et al. 2002) that was grown under a number of growth conditions, and though cells were not always motile during stages of their light/dark cycle, they were always observed to be planktonic and to divide in the planktonic state. We never observed settled cells, a benthic stage or any kind of multi-celled, planktonic colony that might possess microrhizoids.

TEM observations of cell structure and the scale covering. Both flagellate and benthic cells had a single, deeply lobed, cup-shaped chloroplast that enclosed most of the cytoplasm. Lobes were connected by a thin isthmus containing an eyespot comprised of a single layer of lipid granules (Figs. 2c,g-j, 4a-d) and each lobe possessed a large pyrenoid with a thick starch shield. One or more narrow pyrenoid peduncles were occasionally seen penetrating the starch shield between the chloroplast and the pyrenoid (not shown). A small microbody is found opposite the eyespot at the surface of the chloroplast isthmus on the dorsal side of the cell (Fig. 4b). The flattened ventral surface of the cell contained the basal bodies (Fig. 4d,f), which nucleated either flagella or microrhizoids, and a single Golgi stack (Fig. 4d,f) with Golgi-derived vesicles containing developing scales (Fig. 4d,e). Scales covered the entire cell surface (Fig. 4a-d,f), while stacks of scales accumulated at the distal face of the Golgi stack, and on the ventral cell surface, the apparent site of secretion. (Fig. 4f).

Only one type of scale was observed in *M. pickettheapsiorum* and a single layer covered both the surface of the flagella and the cell body of flagellates, while scales were observed to accumulate on the surface of benthic cells. The occasional scale was observed scattered at the base of microrhizoids, but scales were not found along their length (see below). Scales had the same general structure, were very

thin, circular or slightly oblong and 280 nm - 310 nm in diameter. Each scale was composed of between 10–14 concentric ridges (Fig. 5a,b,d) with an outermost thickened rim, while the narrow circumference of the inner 2-3 ridges appeared as a central dot (Fig. 5d). Scales vary only slightly in size over the cell and flagella surfaces. Body scales formed a single layer (Fig. 5c,e) on flagellates, except at the site of secretion as described above. Benthic cells may have several layers of scales that apparently build up over time. (e.g., Fig. 5b).

In flagellates, approximately a third to half of each scale actually adhered to the plasma membrane by an apparent adhesive of varying thickness (Fig. 5b,c,e), the rest of each scale projected off the cell surface as a scoop, or like a sail in thin section, depending on the orientation of the section (Fig. 5c,e). A similar construction was seen on the flagella surfaces, though the scales were imbricated with 8 precise rows of spiraling, overlapping scales inclosing each flagellum (Fig. 6a-e). As above, less than half of each circular scale is adhered to the flagella surface (Fig. 6d,e) the remaining scale forming a scoop-like structure (Fig. 6a-e). Flagella hairs, which are common in *Dolichomastix* (Throndsen & Zingone 1997), were not observed in *M. pickettheapsiorum*, either on whole mounts or material sectioned during flagellate/flagella formation.

Ultrastructure of the flagella apparatus and microrhizoids. The structure of the basal bodies and the associated flagella apparatus was the same for flagellates and benthic cells, though the orientation of the basal bodies was at an acute angle to the ventral cell surface for flagella (Figs 2d, 4d, 7a), and generally perpendicular to the cell surface for microrhizoids (Figs 2l-n, 7b). The orientation of the flagella roots was adjusted accordingly. The long basal bodies and transition region were typical of the Mamiellophyceae (Figs 7a-i) and many green algae and have two transitional plates (Fig. 7c-i). The basal bodies give rise to either a flagellum containing a standard 9+2 axoneme (Fig. 6d,e) or, alternatively, a microrhizoid that typically contains only 9 evenly spaced microtubules (no doublets or central microtubules) over most of their length (Fig. 7i-l). Towards the tips of the microrhizoids a smaller, variable number of microtubules were found (not shown). Flagella were distinguished by a covering of imbricated scales over their entire length (Figs 6a-e, 7a), while the microrhizoids are devoid of scales over most of their length, though scattered scales may be found near the bases of the microrhizoids (Fig. 7c,j).

The flagellar apparatus was not thoroughly investigated, but several details were observed (Figs 8a-i, 9). The two flagella emerged from the ventral surface and extended beyond the posterior end of the cell, passing over a shallow flagellar depression (Figs 2d, 4d,f). When viewed from the cell's ventral to dorsal surface, or from flagellar tips to basal bodies, the longer mature flagellum (1) was on the right and the immature flagellum (2) was on the left (Figs 2d, 9). The immature flagellum was nearly parallel with the

flagellar depression whereas the mature flagellum was tilted slightly toward an axis perpendicular to the flagellar depression.

The basal bodies were attached by a thick, dense distal fiber located just below the flagellar transition zone (Figs 8a,c-e,h, 9) and by a much smaller, proximal fiber at the proximal ends of the basal bodies (Figs 8a,b, 9). In addition, the basal bodies were attached to the plasma membrane with transitional fibers (Fig. 7f,g).

There were at least three microtubular roots (root nomenclature follows Moestrup 2000) (Figs 8a-h, 9). The R1 root originated almost perpendicular to the mature flagellum's basal body approximately midway along the length of that basal body (Figs 8a,b,d, 9), and consisted of two microtubules embedded in a dense material at its nucleation site on the basal body (Fig. 8b,d), and extended to, and then along the plasma membrane (Fig. 8f) and was approximately 300 nm in length. The R2 root originated near the base of the mature basal body and near the proximal fiber (Fig. 8b-d,h). The R2 root consisted of 3 microtubules associated with a dense material near its origin (Fig. 8e), becoming 2 microtubules as the R2 root extended away from the mature basal body at approximately a 30°angle, and passed beneath (to the dorsal side of) the distal fiber (Figs 8c,h, 9), and then extended just beneath the plasma membrane as it curved away toward the right (Figs 7a, 9). The R3 root arose on the left side of the immature basal body (Fig. 8a,b,d), appeared to have 3 microtubules near its origin and extended out to beneath the plasma membrane where 3 microtubules in cross section were observed (Figs 8g, 9). The exact path of R3 and its length was not determined, and an R4 root was not observed.

In addition to the microtubular roots, there was a thin striated fiber that extended from the proximal end of the immature flagellum toward the nuclear envelope (Figs 8i, 9).

DISCUSSION

Our phylogenetic results based on chloroplast genome data and 18S rDNA sequences of cultured strains and environmental samples all agree that *Microrhizoidea* forms a distinctive lineage within the Dolichomastigales. The phylogeny based on chloroplast genome data (Fig. S2) clearly shows that its closest described relative is *Dolichomastix tenuilepis*, which is in agreement with the 18S rDNA trees (Fig. 1, Figs S3,S4) although trees often show undescribed lineages (i.e., environmental sequences) that may be more closely related. The phylogenetic divergence between *Microrhizoidea* and *Dolichomastix* (cf. Fig. S2) is similar to other prasinophyte genus pairs (e.g. *Ostreococcus-Bathycoccos*, *Cymbomonas-Pyramimonas*), suggesting that in combination with its divergent morphological features, *Microrhizoidea* should be recognised as a genus separate from *Dolichomastix*. While the chloroplast genome data provide

clear evidence for the *Microrhizoidea-Dolichomastix* sister relationship, the deeper relationships within the Mamiellophyceae are not well resolved. This is likely due in large part to two critical species (*Crustomastix* and *Dolichomastix*) not having had their complete chloroplast genomes sequenced. The transcriptome-derived data yielded an incomplete matrix with 8 genes for *Crustomastix* and 11 for *Dolichomastix* (out of 69 genes in total), leading to uncertainty about the relationships among Mamiellophyceae lineages. We expect that these relationships will be clarified when more complete datasets become available.

The discovery of *Microrhizoidea* confirms that many divergent lineages can be found in benthic marine habitats (see also Kai *et al.* 2008, Zechman *et al.* 2010, Grant *et al.* 2011, Grant *et al.* 2013, Wetherbee *et al.* 2015, Wetherbee & Verbruggen 2016, Wetherbee *et al.* 2019). Like many other sand-dwelling algae, *M. pickettheapsiorum* has adapted to maintain its place in a dynamic habitat with alternating benthic and short-lived planktonic stages (see below). The phylogenetic position of *Microrhizoidea* in a largely planktonic lineage suggests that in this case the adaptation to benthic habitats was relatively recent, but there certainly are examples of much more ancient transitions of planktonic algae into this habitat, leading to the discovery of new order- and class-level lineages in benthic habitats (e.g. Kai *et al.* 2008, Zechman *et al.* 2009, Wetherbee *et al.* 2019). It is worth noting that many of the lineages in our 18S rDNA phylogenies are only known from planktonic environmental sequences, but one should not dismiss the possibility that more of these lineages have alternating benthic and planktonic stages, and it would be highly informative to have more environmental 18S rDNA surveys of benthic habitats, as the great majority of the work done to date has been on plankton.

It is clear from the environmental 18S rDNA sequences (Monier et al 2015, 2016, Tragin & Vaulot 2018, 2019, this study) that our knowledge of the biodiversity of the Mamiellophyceae is in its infancy, and that the known culture strains represent only a tiny fraction of the actual biodiversity. While pico-sized representatives (< 2 μm in diameter) from the order Mamiellales dominate the biomass in many locations, and are far better known, the nano-sized representatives (2 – 6 μm in diameter) from the order Dolichomastigales comprise significantly more sequence diversity in the Mamiellophyceae (Fig. 1). However, representatives of the latter order have not been well characterized (Marin & Melkonian 2010, Monier et al 2016), and need to be studied in more detail in order to understand the overall role of the Mamiellophyceae in prasinophyte biodiversity and global primary production.

Novel features of M. pickettheapsiorum. This is the first report of a marine flagellate from the Mamiellophyceae, as well as most prasinophytes, found to alternate with a benthic stage that dominates the life cycle. Being sand-dwelling, *M. pickettheapsiorum* has classic mechanisms for adapting to a dynamic habitat, possessing an adhesive benthic stage where cell division occurs, plus the formation of a

short-lived flagellate stage to settle and populate new territory. The utilization of basal bodies for the generation of both flagella for motility and microrhizoids for adhesion has not been observed before, either in another green alga or any other protist.

Microrhizoidea and *Dolichomastix* are presently the only two genera to be described for the Dolichomastigaceae (Fig. 1), and along with *Crustomastix* the only three described representatives of the order Dolichomastigales. Of the four recorded species of *Dolichomastix*, only *D. tenuilepsis* has been cultured, sequenced and described in detail (Throndsen & Zingone 1997, Zingone et al. 2002). The original three species were distinguished only by scale morphology, as observed from whole mounts established from field samples (Manton 1977), satisfactory at the time but no longer a definitive characteristic. The type species *D. nummulifera,* as well as *D. tenuilepsis,* both have thin, circular scales with a delicate pattern of concentric ridges, while the other two species, *D. lepidota* and *D. eurylepidea,* have spider-like scales. Only when the remaining three species of *Dolichomastix* are cultured and sequenced will their relationships be determined. For example, it is possible that the two species distinguished by spider scales will not be included within *Dolichomastix*. While *D. tenuilepsis* and the flagellate of *M. pickettheapsiorum* have similar scales and other similarities in cell structure, a number of morphological features, as well as their divergence in molecular phylogenies indicate that they should be recognised as separate genera. In terms of their life cycles, there is a profound difference.

Basal bodies nucleate flagella and microrhizoids. Basal bodies are protein structures that act as a microtubule organizing center (MTOC) for the nucleation and growth of axoneme microtubules in eukaryotic flagella, and in the case of *M. pickettheapsiorum,* microrhizoids that do not possess a classic axoneme. Although the fundamental structure of flagella in protists is the same, diverse arrays of surface appendages define many taxonomic groups, including flagella hairs, mastigonemes and one or more layers of organic scales in either loose or meticulous orientations. *M. pickettheapsiorum* flagella are characterized by being tightly encased in 8 precise rows of imbricated scales, as are the flagella of *D. tenuilepsis* (see Fig. 30, Throndsen & Zingone 1997). In addition to flagella scales, body scales are synthesized and deployed onto the surface of both flagellates and benthic cells in *M. pickettheapsiorum*, but no scales are deployed onto the microrhizoids, despite the fact they are also nucleated by basal bodies and juxtaposed to the Golgi stack.

Once *M. pickettheapsiorum* flagellates settle and quickly withdraw their flagella, the benthic cells differentiate in one of two ways, either enlarge, divide and produce two new flagellates that detach, or differentiate into the benthic stage, the basal bodies generating two microrhizoids instead of flagella. The

conversion from motile zoospore to benthic sedimentary phase is perhaps not a major drain on cell resources. The two flagella are ~30µm long, each with a canonical 9 + 2 microtubular axoneme extending the full length. If we assume the two flagella are quickly and successfully resorbed (Figs 2e-h; video at https://youtu.be/Vq-ZgU2nn90), and the constitutive proteins and membrane lipids recycled, the cell could potentially use these building blocks to help generate the two microrhizoids, which can take up to 48 hours to reach full length. The microrhizoids are variable in length but commonly less than 100µm. Thus, the cell could have tubulin resources from two 30µm axonemes to devote to the microtubules in the microrhizoids. Given that an axoneme comprises 20 microtubules (nine doublets plus the central pair) while the microrhizoids typically have 9 singlet microtubules, we estimate that the tubulin from the flagella could service about two thirds of the building blocks for the microtubules in two 100µm microrhizoids. Similarly, the membrane lipids from the two flagella, which are about the same diameter as the two microrhizoids, could provide about 30% of the requirements for membrane lipids. Obviously, the energy used to dismantle the flagella and then muster the released resources into microrhizoid biogenesis would not be insubstantial, so the sedimentary lifestyle must offer a substantial advantage to repay all these resources.

Pseudoflagella in the green algae. The vegetative cells of several freshwater, colonial genera from the Tetrasporaceae (Chlorophyceae), including *Tetraspora* (Lembi and Walne 1971) and *Octosporiella* (Kugrens 1984), possesss two pseudoflagella (referred to by the author as pseudocilia) generated from the basal bodies in a similar fashion to the microrhizoids of *M. pickettheapsiorum*. Pseudoflagella are stiff, short and radiate out beyond the boundaries of the colonies that are typically planktonic. The ultrastructure of pseudoflagella is similar to microrhizoids, however pseudoflagella are relatively very short and do not arise following the settlement and adhesion of individual zoospores, nor do they attach the non-motile cells or colonies to the substratum. The large spherical colonies that characterize the Tetrasporales are symmetrical and well organized, and often adhere together in an irregular mass. Alternatively, *M. pickettheapsiorum* colonies are less ordered and much smaller, generally consisting of only 16-32 cells, strongly adhered to the substratum by microrhizoids and with cells that can differentiated into motile flagellates with standard flagella. Tetrasporean colonies do produce zoospores, but with short, stiff pseudoflagella rather than flagella, so motility appears lost in this group of green algae.

Protist appendages not nucleated by basal bodies. Some protists are endowed with additional appendages that are nucleated by MTOCs other than basal bodies and have a range of complex functions. For example, the haptonema of many mixotrophic prymnesiophytes possesses 6-7 interconnected microtubules nucleated by an MTOC within the flagella apparatus, but not by a basal body (e.g., Manton 1964). The haptonema in some species has a key role in pray capture during phagocytosis, but in other

species appears to function in surface adhesion and/or prey avoidance responses (Kawachi et al 1991). Even more spectacular are the elongate tentacles of *Apedinella* (Dictyochophyceae, Heterokonta) that contain a triad of interconnected microtubules nucleated on the nuclear envelope, and participate in the control and orientation of large, extracellular organic spines in a series of complex movements (Koutoulis et al. 1989). Additional appendages supported by various numbers of microtubules that nucleate off the nuclear envelope are common in species of the Dictyochophyceae (Moestrup & Thomsen 1990. Swale, E.M.F. 1969). For example, tentacles, rhizopodia and the trailing peduncle of *Pedinella* and related genera consist of several microtubules (generally 5-10). While their function is not always clear, peduncles are involved in the adhesion of cells to the substratum. Microtubule associated proteins are common in all these appendages (e.g., Koutoutlis et al. 1989).

Flagella apparatus. The long basal bodies and flagellar transition regions (transitional helix and plate) of *M. pickettheapsiorum* have the same characteristics as several prasinophyte species, including from the Mamiellophyceae, such as *Mamiella gilva* (Parke et Rayns) Moestrup (Moestrup 1984), *Crustomastix stigmatica* Zingone (Zingone et al. 2002) and *D. tenuilepsis* (Throndsen & Zingone 1997). Studies of the flagella apparatus in the three described genera of the Dolichomastigales are incomplete at best, and therefore comparison of reconstructions are of no value in determining evolutionary relationships.

TAXONOMIC TREATMENT

Microrhizoidea pickettheapsiorum Wetherbee**, gen. et sp. nov.**
Type species – Microrhizoidea pickettheapsiorum Wetherbee

Combined genus and species description. Flagellates were rounded to bean shaped, 5.0 -6.5 μm in width and 6.0 - 7.5 μm in length including the scale covering (Fig. 2 a-c), flattened laterally where the two flagella are inserted (Fig. 2d) at an acute angle to the cell surface. The chloroplast is deeply lobed (e.g., Fig. 2c), each lob contained a distinctive pyrenoid with accompanying starch shield (Fig. 2a,b,h,i). The two flagella were between 3.5-5 times the length of the cell (25 - 35 μm) (Fig. 2a,b) with one flagellum being slightly longer than the other. One type of scale covered both the surface of the flagella and cell body. Scales were circular, occasionally oblong, and very thin, 280 nm in diameter. Scales on the flagella surfaces were imbricated with 8 rows of spiraling, overlapping scales. Less than half of each circular scale is adhered to the flagella surface, the remaining scale forming a scoop-like structure. Flagella hairs were not observed in either whole mounts or TEM images. Flagellates settled (Fig. 2e-i), produced two, long anchoring microrhizoids using the flagella basal bodies as organizing centers (Figs 2i-n, 3a-c), and then divided (Fig. 2j,k). The daughter cells either returned to the flagellate stage or started a benthic palmelloid colony. Microrhizoids were scale-less, stiff and never beat. Benthic colonies became encased

in a mucilagenous covering while daughter cells at the colony's interface with the media often differentiated into flagellates, growing flagella rather than microrhizoids. Flagella had a prominent scale covering (0.5–0.6 μm) while the scale-less microrhizoids (c. 0.2 μm) were thinner. The basal bodies that generate flagella were at an acute angle to the cell surface, and the flagella began to beat almost immediately. In culture, flagellates that did not find a surface for attachment formed planktonic, palmelloid colonies with microrhizoids that were diminished and never appeared to leave the mucilaginous covering. Sexual reproduction was not observed.

Holotype – MELU A TasT39, a mounted specimen derived from strain CS-1218, collected January, 2009, from sand between high intertidal rocks, by Brenna Grant.

Type locality – Trial Bay, approximately 20 m East of the jetty, Tasmania, Australia (43° 07' 54"S; 147° 15' 19"E).

Genbank accession numbers – Strain CS-1218: _____; CS-1267_____; CS-1268____; CS-1269_____.

Etymology – The genus describes a sand-dwelling prasinophyte with a benthic stage that adheres by novel microrhizoids (i.e., *Microrhizoidea*). The specific epithet is a plural noun in the genetive case honouring Jeremy David Pickett-Heaps and Julianne Pickett-Heaps for their outstanding video documentation of the morphology and development of algae, particularly the green algae of which *M. pickettheapsiorum* is a member. Their teaching and research videos (https://www.cytographics.com) have thrilled and inspired generations of undergraduate and postgraduate students, as well as microscopists and naturalists the world over.

Habitat – marine, sand-dwelling.

Culture lodgement – ANACC code: Tas T39, Tasmania CS-1218; 5FNG, West Australia strain CS-1267; NB3, Queensland strain CS-1268; Wye4, Victoria strain CS-1269; CSIRO, Hobart, Tasmania, Australia.

Acknowledgements: We thank Allison van de Meene, the School of Biosciences Microscopy Unit at the University of Melbourne, for the use of the electron microscopes and accessory equipment. We thank Adam Monier for providing the OTU sequences associated with Monier et al. (2016). Financial support was provided by the Australian Research Council (DP150100705) and the University of Melbourne Botany Foundation.

References:

Abascal, F., Zardoya, R. & Telford, M. J. 2010. TranslatorX: multiple alignment of nucleotide sequences guided by amino acid translations. *Nucleic Acids Res.* 38:W7-W13.

Beck, N. & Lang, B. F. 2010. MFannot, organelle genome annotation webserver. http://megasun.bch.umontreal.ca/RNAweasel/.

Bork, P., Bowler, C., de Vargas, C., Gorsky, G., Karsenti, E., Wincker, P. (2015) Tara Oceans studies plankton at planetary scale. *Science* 348: 873

Cremen, M. C. M., Huisman, J. M., Marcelino, V. R. & Verbruggen, H. 2016. Taxonomic revision of *Halimeda* (Bryopsidales, Chlorophyta) in south-western Australia. *Austr. Syst. Bot.* 29:41-54.

Cremen, M. C. M., Leliaert, F., Marcelino, V. R. & Verbruggen, H. 2018. Large diversity of nonstandard genes and dynamic evolution of chloroplast genomes in siphonous green algae (Bryopsidales, Chlorophyta). *Genome Biol. Evol.* 10:1048-61.

Cremen, M. C. M., Leliaert, F., West, J., Lam, D. W., Shimada, S., Lopez-Bautista, J. M. & Verbruggen, H. 2019. Reassessment of the classification of Bryopsidales (Chlorophyta) based on chloroplast phylogenomic analyses. *Mol. Phylogen. Evol.* 130:397-405.

Edgar, R. C. 2004. MUSCLE: multiple sequence alignment with high accuracy and high throughput. *Nucleic Acids Res.* 32:1792-7.

Fučíková, K., Leliaert, F., Cooper, E. D., Škaloud, P., D'hondt, S., De Clerck, O., Gurgel, C. F. D., Lewis, L. A., Lewis, P. O., Lopez-Bautista, J. M., Delwiche, C. F. & Verbruggen, H. 2014. New phylogenetic hypotheses for the core Chlorophyta based on chloroplast sequence data. *Frontiers Ecol. Evol.* 2:63.

Grant, B., Waller, R.F. & Wetherbee, R. 2011. *Platychrysis moestrupii sp. nov.* (Prymnesiophyceae): a new dimorphic, sand-dwelling haptophyte species from southeastern Australia. *Phycologia* 50:608-15.

Grant, B., Waller, R.F., Clementson, L., & Wetherbee, R. 2013. *Psammamonas australis gen. et sp. nov*. (Raphidophyceae), a new dimorphic, sand-dwelling raphidophyte from southeastern Australia. *Phycologia* 52:57-64.

Hanaichi, T., Sato, T., Hoshin, M. & Mizuno, N. 1986. A stable lead stain by modification of Sato's method. *Proc XIth Int. Cong. On Electron Microscopy*, Kyoto. P. 2181-2.

Kawachi, M., Inouye, I., Maeda, O. & Chihara, M. 1991 Thehaptonema as a food-capturing device: observations on *Chrysochromulina hirta* (Prymnesiophyceae). *Phycologia* 30:563-73.

Hoang, D.T., Chernomor, O., von Haeseler, A., Minh, B.Q. & Vinh, L.S. 2018. UFBoot2: Improving the ultrafast bootstrap approximation. *Mol. Biol. Evol.* 35: 518-22.

Jackson, C., Knoll, A. H., Chan, C. X. & Verbruggen, H. 2018. Plastid phylogenomics with broad taxon sampling further elucidates the distinct evolutionary origins and timing of secondary green plastids. *Sci. Rep.* 8:1523.

Johnson, L. K., Alexander, H. & Brown, C. T. 2018. Re-assembly, quality evaluation, and annotation of 678 microbial eukaryotic reference transcriptomes. GigaScience:giy158-giy58.

Kalyaanamoorthy, S., Minh, B. Q., Wong, T. K. F., von Haeseler, A. & Jermiin, L. S. 2017. ModelFinder: fast model selection for accurate phylogenetic estimates. *Nat. Methods* 14:587-89.

Katoh, K. & Standley, D. M. 2013. MAFFT multiple sequence alignment software version 7: improvements in performance and usability. *Mol. Biol. Evol.* 30:772-80

Kearse, M., Moir, R., Wilson, A., Stones-Havas, S., Cheung, M., Sturrock, S., Buxton, S., Cooper, A., Markowitz, S., Duran, C., Thierer, T., Ashton, B., Meintjes, P. & Drummond, A. 2012. Geneious Basic: An integrated and extendable desktop software platform for the organization and analysis of sequence data. *Bioinformatics* 28:1647-9.

Keeling, P. J., Burki, F., Wilcox, H. M., Allam, B., Allen, E. E., Amaral-Zettler, L. A., Armbrust, E. V., Archibald, J. M., Bharti, A. K., Bell, C. J., Beszteri, B., Bidle, K. D., Cameron, C. T., Campbell, L., Caron, D. A., Cattolico, R. A., Collier, J. L., Coyne, K., Davy, S. K., Deschamps, P., Dyhrman, S. T., Edvardsen, B., Gates, R. D., Gobler, C. J., Greenwood, S. J., Guida, S. M., Jacobi, J. L., Jakobsen, K. S., James, E. R., Jenkins, B., John, U., Johnson, M. D., Juhl, A. R., Kamp, A., Katz, L. A., Kiene, R., Kudryavtsev, A., Leander, B. S., Lin, S., Lovejoy, C., Lynn, D., Marchetti, A., McManus, G., Nedelcu, A. M., Menden-Deuer, S., Miceli, C., Mock, T., Montresor, M., Moran, M. A., Murray, S., Nadathur, G., Nagai, S., Ngam, P. B., Palenik, B., Pawlowski, J., Petroni, G., Piganeau, G., Posewitz, M. C., Rengefors, K., Romano, G., Rumpho, M. E., Rynearson, T., Schilling, K. B., Schroeder, D. C., Simpson, A. G. B., Slamovits, C. H., Smith, D. R., Smith, G. J., Smith, S. R., Sosik, H. M., Stief, P., Theriot, E., Twary, S. N., Umale, P. E., Vaulot, D., Wawrik, B., Wheeler, G. L., Wilson, W. H., Xu, Y., Zingone, A. & Worden, A. Z. 2014. The Marine Microbial Eukaryote Transcriptome Sequencing Project (MMETSP): Illuminating the functional diversity of eukaryotic life in the oceans through transcriptome sequencing. *PLoS Biol.* 12:e1001889.

Keller, M. D., Selvin, R. C., Claus, W. & Guillard, R. R. L. 1987. Media for the culture of oceanic ultraphytoplankton. *J. Phycol*. 23:633–8.

Koutoulis, A., McFadden, G.I. & Wetherbee, R. 1988. Spine-scale reorientation in *Apedinella radians* (Pedinellales, Chrysophyceae): the microarchitecture and immunocytochemistry of the associated cytoskeleton. *Protoplasma* 147:25-41.

Kugrens, P. 1984. *Octosporiella coloradoensis* gen. et sp. nov., a new tetrasporalean green alga from two Colorado mountain lakes. *J. Phycol*. 20:88-94.

Laslett, D. & Canback, B. 2004. ARAGORN, a program to detect tRNA genes and tmRNA genes in nucleotide sequences. *Nucleic Acids Res.* 32:11-6.

Lembi, C.A. & Walne, P.L. 1971. Ultrastructure of pseudocilia in *Tetraspora lubrica* (Roth) AG. *J. Cell Sci.* 9:569-579.

Manton, I. 1964. Further observations on the fine structure of the haptonema in *Prymnesium parvum*. *Archiv fur Mikrobiologie* 49:315-30.

Manton, I. 1977. *Dolichomastix* (Prasinophyceae) from Arctic Canada, Alaska and South Africa: a new genus of flagellates with scaly flagella. *Phycologia* 16: 427-438.

Marcelino, V. R., Cremen, M. C. M., Jackson, C. J., Larkum, A. & Verbruggen, H. 2016. Evolutionary dynamics of chloroplast genomes in low light: a case study of the endolithic green alga *Ostreobium quekettii. Genome Biol. Evol.* 8:2939-51.

Marin, B. & Melkonian, M. 2010. Molecular phylogeny and classification of the Mamiellopyceae class. Nov. (Chlorophyta) based on sequence comparisons of the nuclear- and plastid-encoded rRNA operons. *Protist* 161:304-336.

Melkonian, M., Marin, B. & Surek, B. 1995. Phylogeny and evolution of the algae. In Arai, R., Kato, M., & Doi, Y. (eds) Biodiversity and Evolution. The National Science Museum Foundation, Tokyo, pp. 153-176.

Moestrup, Ø. 2000. The flagellate cytoskeleton. Introduction of a general terminology for the microtubular flagellar roots in protists. I. The Flagellates, Unity, Diversity and Evolution. Taylor, London & New York, s. 69-94.

Moestrup, Ø., Hori, T. & Kristiansen, A. 1987. Fine structure of *Pyramimonas octopus* sp.nov., and octoflagellated benthic species of *Pyramimonas* (Prasinophyceae), with strong observations on its ecology. *Nor. J. Bot.* 7:339-52.

Moestrup, Ø. & Thomsen, H.A. 1990. *Dictyocha speculum* (Silicoflagellata, Dictyochophyceae), studies on armoured and unarmoured stages. *Biologiske Skrifter 37*, The Royal Danish Academy of Sciences and Letters. Kommissionaer: Munksgaard, Copenhagen. pp. 1-57.

Monier, A., Sudek, S., Fast, N.M. & Worden, A.Z. 2013. Gene invasion in distant eukaryotic lineages: discovery of mutually exclusive genetic elements reveals marine biodiversity. *ISME J* 7: 1764–74.

Monier, A., Comte, J., Babin, M., Forest, A., Matsuoka, A., & Lovejoy, C. 2015. Oceanographic structure drives the assembly processes of microbial eukaryotic communities. *ISME J* 9: 990–1002.

Monier, A., Worden, A.Z., & Richards, T.A. 2016. Phylogenetic diversity and biogeography of the Mamiellophyceae lineage of eukaryotic phytoplankton across the oceans. *Envir.l Microbiol. Rep*. 8:461-9.

Nguyen, L. T., Schmidt, H. A., von Haeseler, A. & Minh, B. Q. 2015. IQ-TREE: a fast and effective stochastic algorithm for estimating maximum-likelihood phylogenies. *Mol. Biol. Evol.* 32: 268-74.

Not, F, Latasa, M., Scharek, R., Viprey, M., Karleskind, P., Balague, V., et al. 2008. Protistan assemblages across the Indian Ocean, with a specific emphasis on the picoeukaryotes. *Deep Sea Res Part 1: Oceanogr. Res. Pap. 55*: 1456-1473.

Spurr, A. R. 1969. A low-viscosity epoxy resin embedding medium for electron microscopy. *J. Ultrastruct. Res*. 26:3143.

Stamatakis, A. 2014. RAxML version 8: a tool for phylogenetic analysis and post-analysis of large phylogenies. *Bioinformatics* 30:1312-13.

Swale, E.M.F. 1969. A study of the nannoplankton flagellate *Pedinella hexacostata* Vysotskii by light and electron microscopy. *British Phycol. J*. 4: 65-86.

Talavera, G. & Castresana, J. 2007. Improvement of phylogenies after removing divergent and ambiguously aligned blocks from protein sequence alignments. *Syst. Biol.* 56:564-77.

Throndsen, J. & Zingone, A. 1997. *Dolichomastix tenuilepis* sp. nov., a first insight into the microanatomy of the genus *Dolichomastix* (Mamiellales, Prasinophyceae, Chlorophyta). *Phycologia* 36:244-54

Tragin, M. & Vaulot, D. 2018. Green microalgae in marine coastal waters: The Ocean Sampling Day (OSD) dataset. *Sci. Rep.* 8:14020.

Tragin, M. & Vaulot, D. 2019. Novel diversity within marine Mamiellophyceae (Chlorophyta) unveiled by metabarcoding. *Sci. Rep.* 9:5190.

Vaulot, D., Eikrem, W., Viprey, M. and Moreau, H. 2008. The diversity of small eukaryotic phytoplankton. *FEMS Microbiol. Rev.* 32:795-820.

Wetherbee, R., Gornik, S.G., Grant, B. & Waller, R.F. 2015. *Andersenia*, a genus of filamentous, sand-dwelling Pelagophyceae from southeastern Australia. *Phycologia* 54:35-48.

Wetherbee, R. & Verbruggen, H. 2016. *Kraftionema allantoideum*, a new genus and family of Ulotrichales (Chlorophyta) adapted for survival in high intertidal pools. *J. Phycol*. 52:701-15

Wetherbee, R., Jackson, C.J., Repetti, S.I., Clementson, L.A., Costa, J.F., van de Meene, A., Crawford, S. & Verbruggen, H. 2019. The golden paradox – a new heterokont lineage with chloroplasts surrounded by two membranes. *J. Phycol*. 55:257-78.

Worden, A.Z., Nolan, J.K., and Palenik, B. 2004. Assessing the dynamics and ecology of marine picophytoplankton: the importance of the eukaryotic component. *Limnol. Oceanogr.* 49:168–79.

Zechman, F. W., Verbruggen, H., Leliaert, F., Ashworth, M., Buchheim, M. A., Fawley, M. W., Spalding, H., Pueschel, C. M., Buchheim, J. A., Verghese, B. & Hanisak, M. D. 2010. An unrecognized ancient lineage of green plants persists in deep marine waters. *J. Phycol.* 46:1288-95.

Zingone, A., Borra, M., Brunet, C., Forlani, G., Kooistra, W.H.C.F. & Procaccini, G. 2002. Phylogenetic position of *Crustomastix stigmatica* sp. nov. and *Dolichomastix tenuilepis* in relation to the mamiellales (Prasinophyceae, Chlorophyta). *J. Phycol*. 28:1012-39.

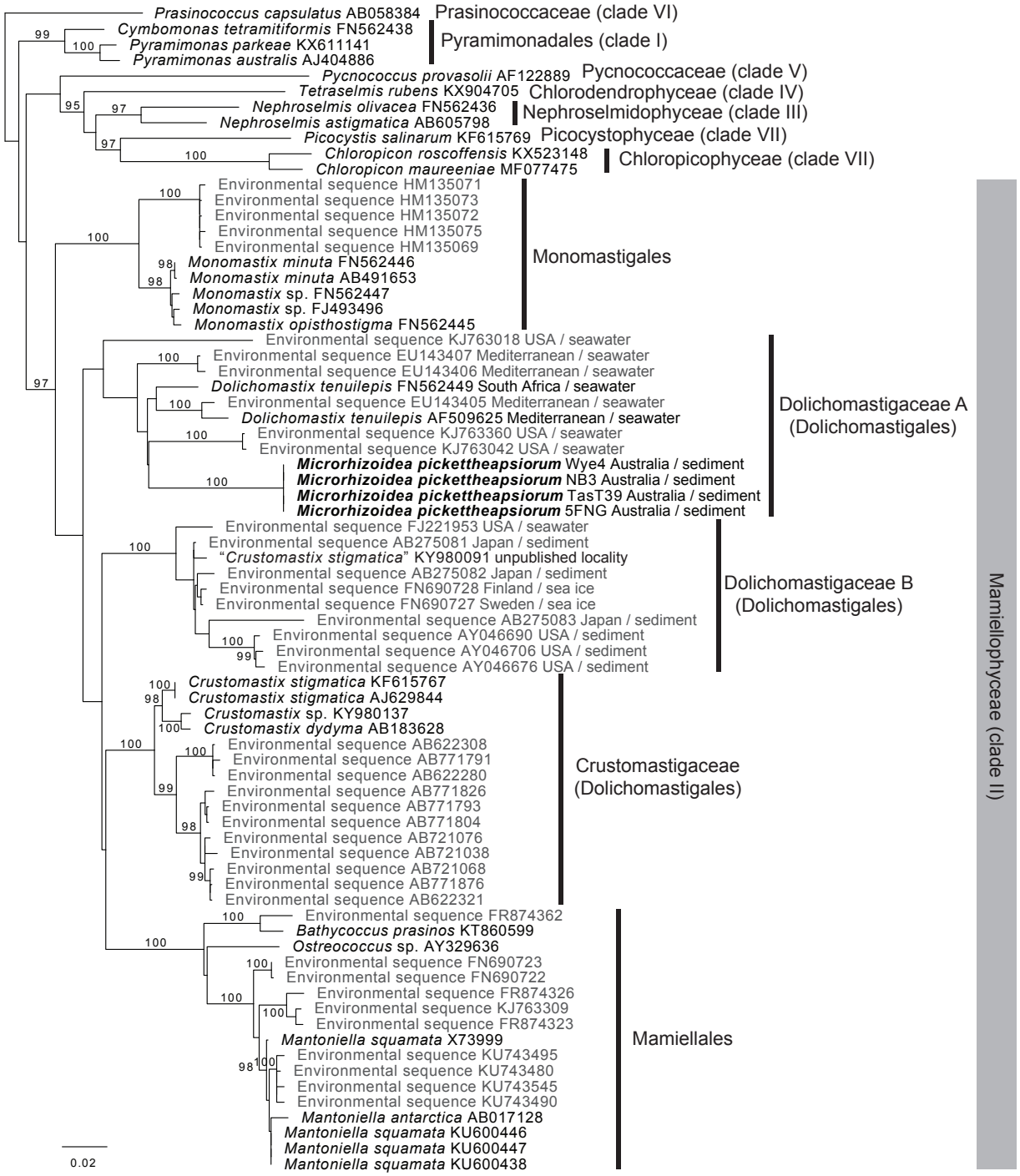

Fig. 1. Maximum likelihood phylogeny of 18S rRNA genes indicating the position of *Microrhizoidea pickettheapsiorum* in relation to other Mamiellophyceae, based on 18S dataset 1. Environmental sequences are indicated in grey. Ultrafast bootstrap values >95% are indicated on the tree nodes.

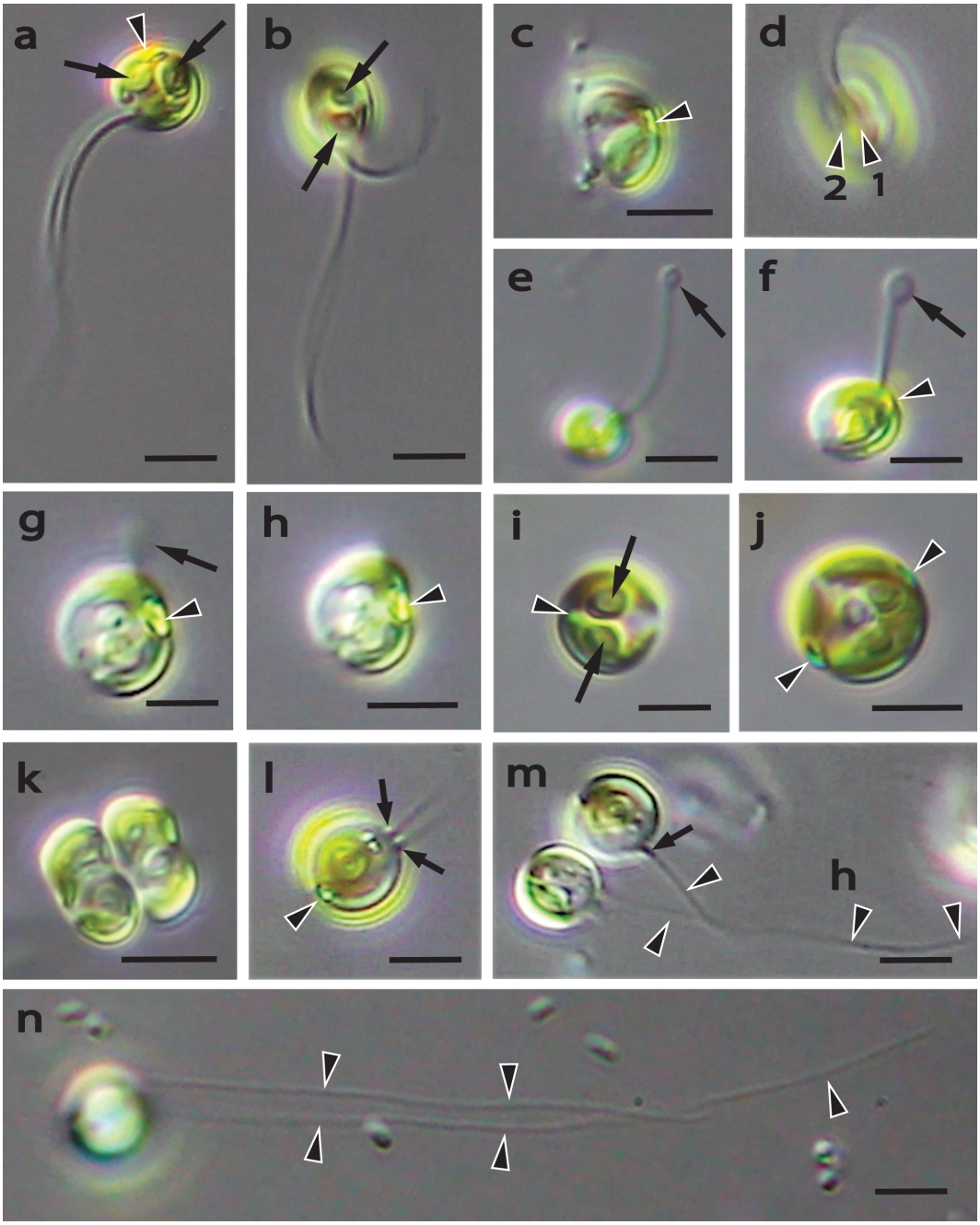

Fig. 2. Light microscope images of *Microrhizoidea pickettheapsiorum gen. et sp. nov*.. (a) Flagellate with two flagella beating together simultaneously, two pyrenoids with starch shields (arrows) in the two lobes of the chloroplast with the eyespot (arrowhead) between. (b) Same flagellate as in (a) in a different orientation, two pyrenoids are observed (arrows). The two flagella beating independently of one another. (c) Same flagellate as in (a, b) in a different orientation. Two lobes of the chloroplast are observed with the eyespot between (arrowhead). (d) Ventral cell surface showing the origin of the flagella. (e - h) Stages in flagellate settlement. Immediately following initial adhesion to the coverslip, the flagella are quickly withdrawn into the cell. The scale covering is presumably left behind and accumulates at the tip of the retracting flagellum (arrow). A flattened benthic cell results with the eyespot (arrowhead) between the chloroplast lobes. (h) Benthic cell with withdrawn flagella; cup-shaped chloroplast with pyrenoids/starch shields (arrows) and the eyespot (arrowhead) located at the bridge between the two chloroplast lobes. (i - k) Settled benthic cells enlarge and the chloroplast with pyrenoids (arrows) and eyespot (arrowheads) are duplicated prior to division. (l) Recently established benthic cell has started to produce two thin microrhizoids perpendicular to the cell surface, one from each basal body (arrowheads). (m, n) Benthic cells are producing long, thin microrhizoids (arrowheads) from basal bodies (arrow). Not all basal bodies and microrhizoids are in the plane of focus. Scale bars = 5.0 μm (a – n)

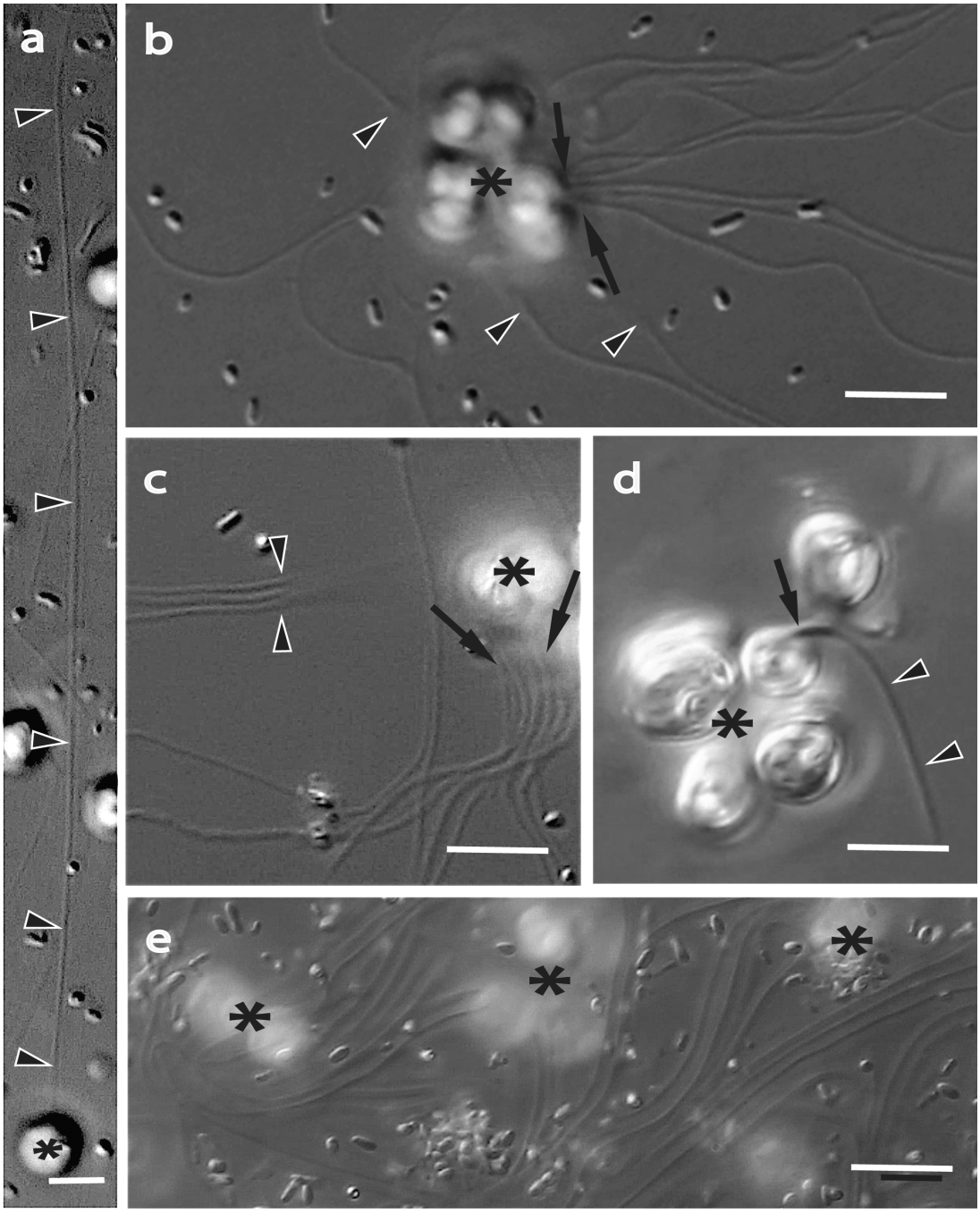

Fig. 3. Light microscope images of the benthic cells of *Microrhizoidea pickettheapsiorum gen. et sp. nov*.. settled on coverships. Some bacteria are also observed. (a) One of two microrhizoids (arrowheads) of a benthic cell (asterisk) is straight and over 95 µm in length. (b, c) Following several division cycles, adhered benthic colonies (asterisk) have formed on the surface of the covership and are immersed in a mucilaginous covering. Microrhizoids originating from the basal bodies of each cell grow until they hit the substratum and then extend out from the colony. Microrhizoids originating from cells attached directly to the substratum are seen extending out directly from beneath the colony (arrows). Microrhizoids generated from cells positioned above the substratum often meet the coverslip some distance from the colony (arrowheads), before they adhere and extend further. (d) Daughter cells on the surface of colonies may form flagellates, generating flagella (arrowheads) at a low angle to the cell surface (arrow). Flagella, which start to beat immediately, are covered by scales and are therefore thicker than microrhizoids and easy to identify. (e) In mature cultures, microrhizoids dominate the coverslip surface while the colonies (asterisk) don't increase much in size, producing more flagellates than benthic cells. Scale bars = 5.0 µm (a), 10.0 µm (b – e).

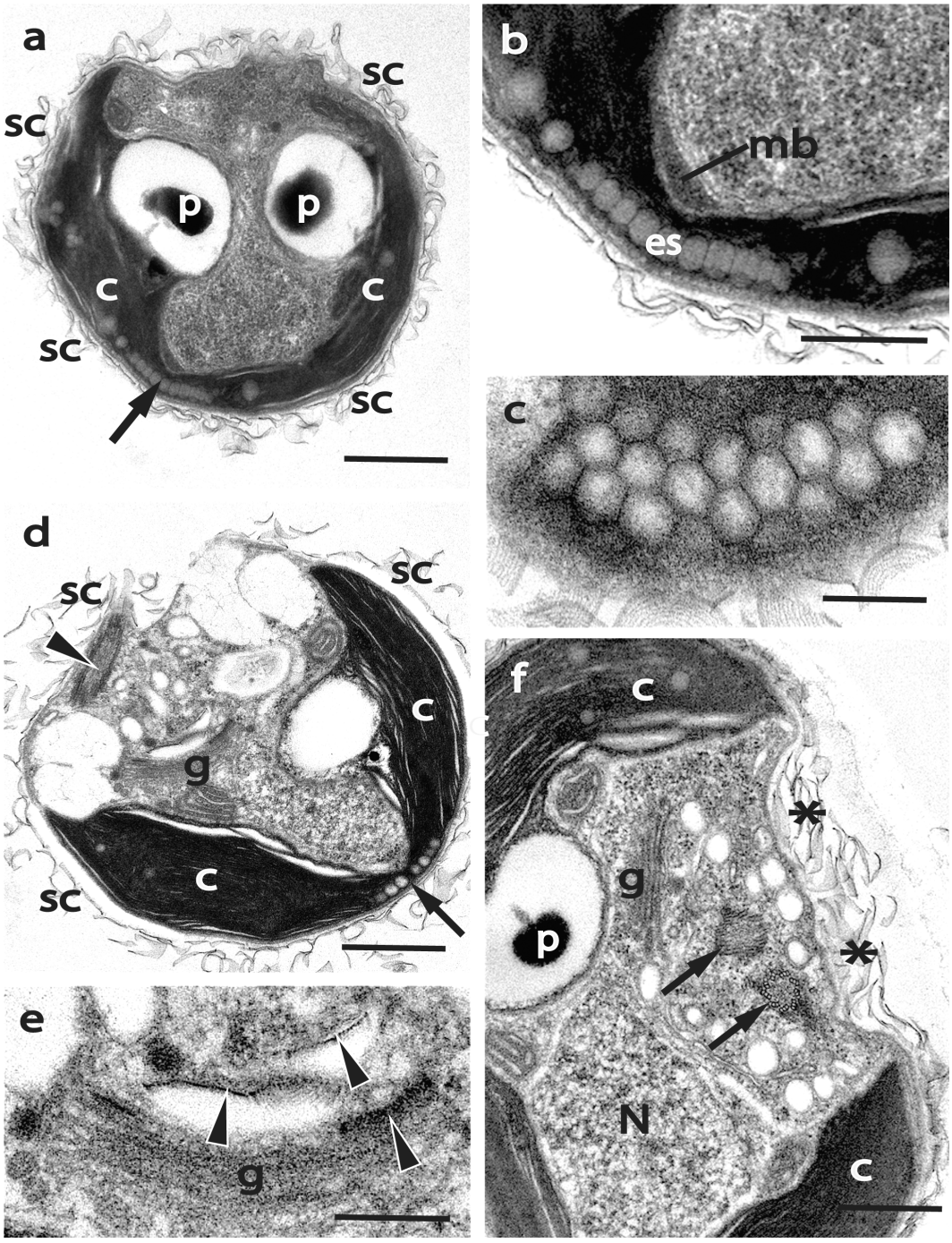

Fig. 4. TEM images (a – f) of the cells of *Microrhizoidea pickettheapsiorum gen. et sp. nov.*. (a) Benthic cell showing the cup-shaped chloroplast with two lobes connected by a narrow bridge containing the eyespot (arrow) and each lobe containing a pyrenoid (p) with a thick starch shield. The scale covering (sc) surrounds the cell. (b). Close-up from figure (a) showing the single layered eyespot (es) within the chloroplast and adjacent to a small microbody (mb), both on the dorsal surface. (c) Eyespot shown in tangential section. (d, e) Section through a flagellate showing the cup-shaped chloroplast with connecting bridge between the two lobes containing the eyespot (arrow), scales (sc) cover the surface. The ventral surface shows a basal body (arrow) oriented at a low angle to the cell surface, a single large Golgi stack (g) seen in close-up (figure e) producing scales (arrowheads). (f) Ventral surface of a benthic cell showing two chloroplast lobes (c), nucleus (N), a pyrenoid with starch shield (p), a Golgi stack (g) and a cross-section of two basal bodies (arrows). Scales are released on the ventral surface adjacent to the distal face of the Golgi, and appear to be secreted in mass in this region (asterisk). Scale bars = 1.5 μm (a, c), 1.0 μm (b), 0.5 μm (d, f), 0.4 μm (e).

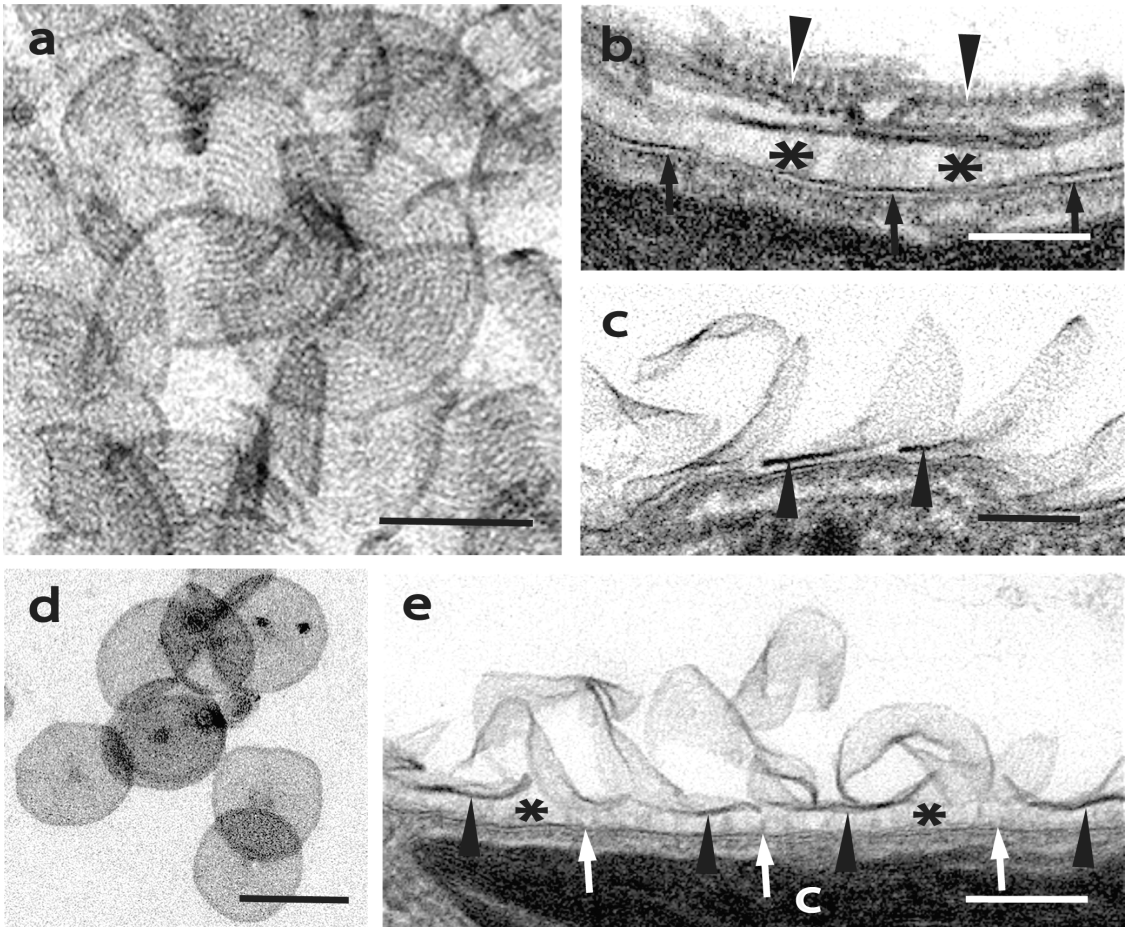

Fig. 5. TEM images (a – e) of the scales of *Microrhizoidea pickettheapsiorum gen. et sp. nov*.. (a) Tangential section through body scales in stacks on the ventral cell surface. Scales 280-310 nm in diameter composed of 10-14 concentric ridges with a thicker, outer rim. (b) Stacked scales on the surface of a benthic cell buried within a colony showing the scale ridges in cross-section (arrowheads). Scales attached to the plasma membrane (arrows) by an adhesive layer (asterisks). (c) Single layer of body scales (arrowheads) is attached to the plasma membrane. Scales project off the surface to form scoop-like structures that look like sails in thin section. (d) Whole mount of body scales. (e) Scales attached (arrowheads) in a single layer over most of the cell surface above the plasma membrane (arrows) and adhesive layer (asterisks). The non-attached regions of the scales projected off the plasma membrane surface and the orientation of the section determined their appearance. Scale bars = 150 nm (a, c, e), 300 nm (b, d).

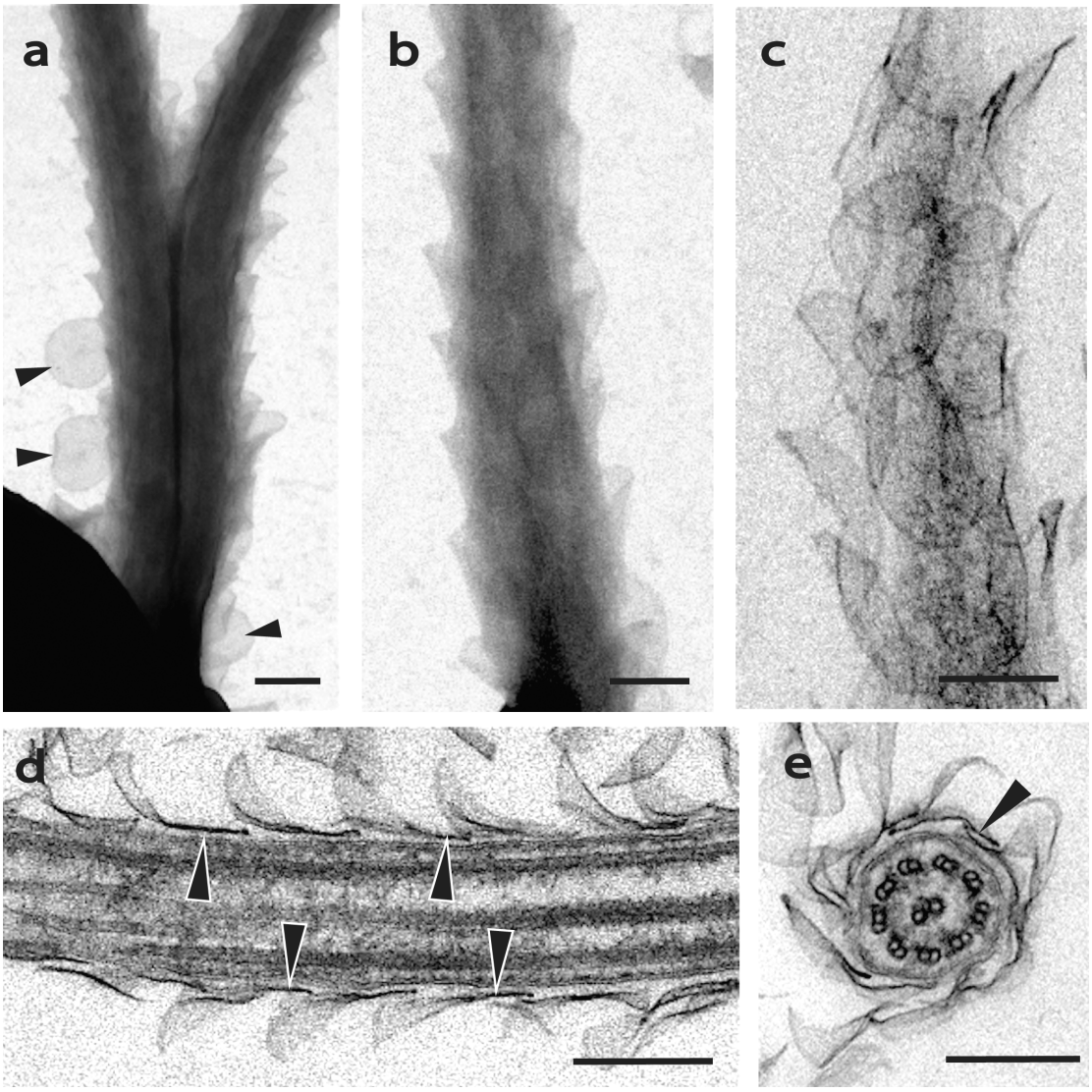

Fig. 6. Whole mount and TEM images (a – e) of the flagella and flagella scales of *Microrhizoidea pickettheapsiorum gen. et sp. nov*.. (a, b) Whole mounts of flagella covered in closely aligned, imbricated scales in rows of 8. Some scales have fallen off and are circular (arrowheads). (c) Glancing TEM section of a flagellum showing the overlapping rows of imbricated scales. (d) Longitudinal TEM section through the center of a flagellum. Scales are in imbricated rows, a region of each scale attached to the flagella membrane (arrowheads) the remaining part of each scale projecting off the surface as a scoop. (e) TEM cross-section of a flagellum showing the classic 9 + 2 axoneme and the 8 overlapping scale rows (arrowhead). The flagella are 24 μm in diameter but the overall diameter including the scale covering is over 50 μm. Scale bars = 25 μm (a – e).

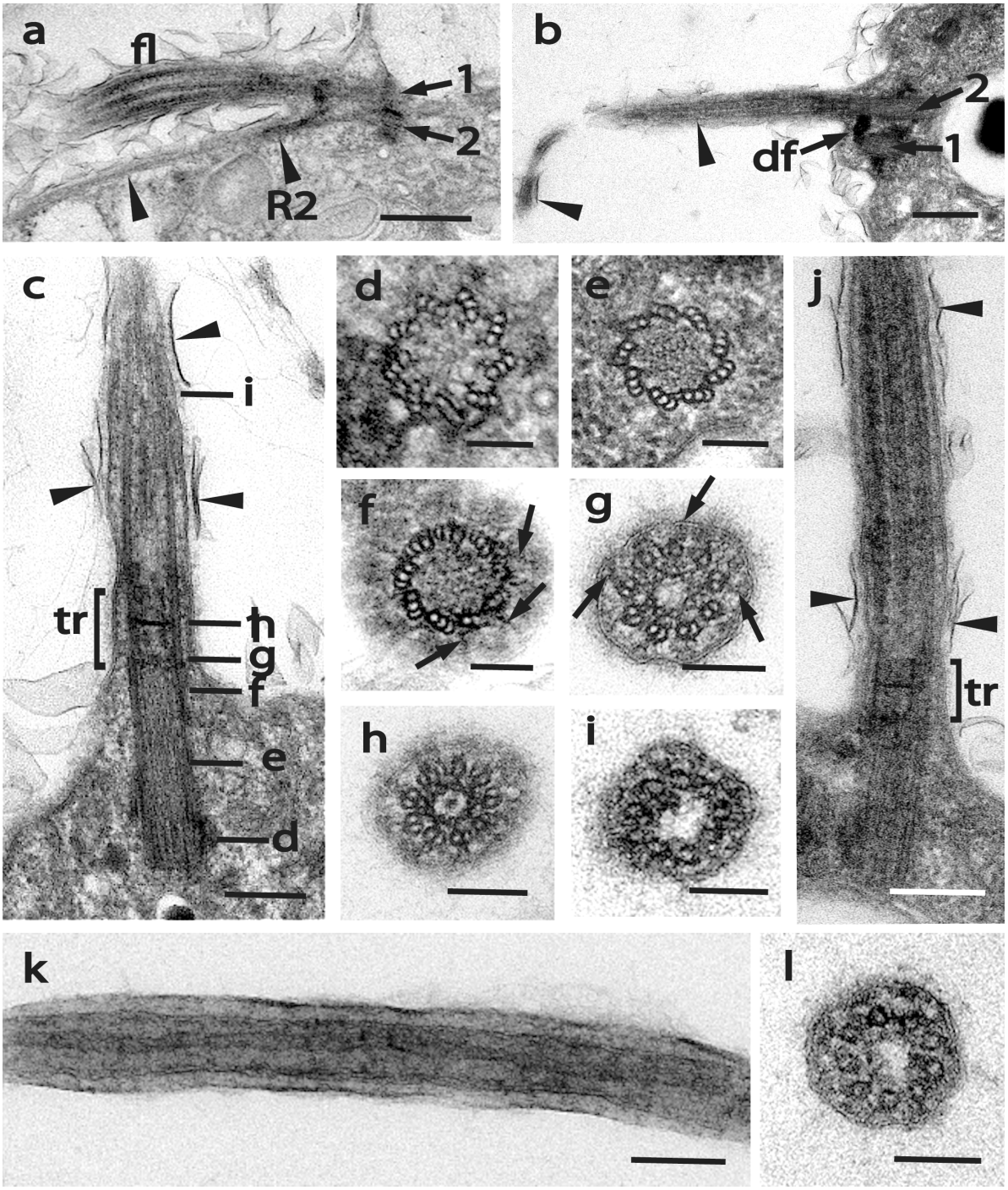

Fig. 7. TEM images (a – l) of the basal bodies and microrhizoids of *Microrhizoidea pickettheapsiorum gen. et sp. nov.*. (a) Glancing section through the two basal bodies (1 and 2) and one of the two flagella (fl) that are orientated at an acute angle to the ventral cell surface. Flagella are covered in scales. The R2 microtutular root (arrowheads) originates from basal body 1 (see figs 8 and 9) and extends out beneath the surface of the plasma membrane. (b) Low magnification image showing a microrhizoid (mr, arrowheads) that develops perpendicular to the benthic cell surface and does not have a scale covering. Both basal bodies (1 and 2) and elements of the flagella apparatus are shown in glancing section (df = distal fiber). (c and j) Longitudinal sections through basal bodies showing the transition region (tr) that has produced a microrhizoid, which has only a few scattered scales (arrowheads) near the base of the microrhizoid. (d – i) Transverse sections at the basal body/microrhizoid levels indicated by the lines (d – i) in figure (c), revealing the basal body (d – f), transition region (g, h) and microrhizoid (i). (k and l) Structure of microrhizoids in both longitudinal and cross section. Note the 9 individual microtubules that characterize microrhizoids (i and l). Scale bars = 50 μm (a), 40 μm (b), 25 μm (c), 12 μm (d – h), 10 μm (i, l), 20 μm (k).

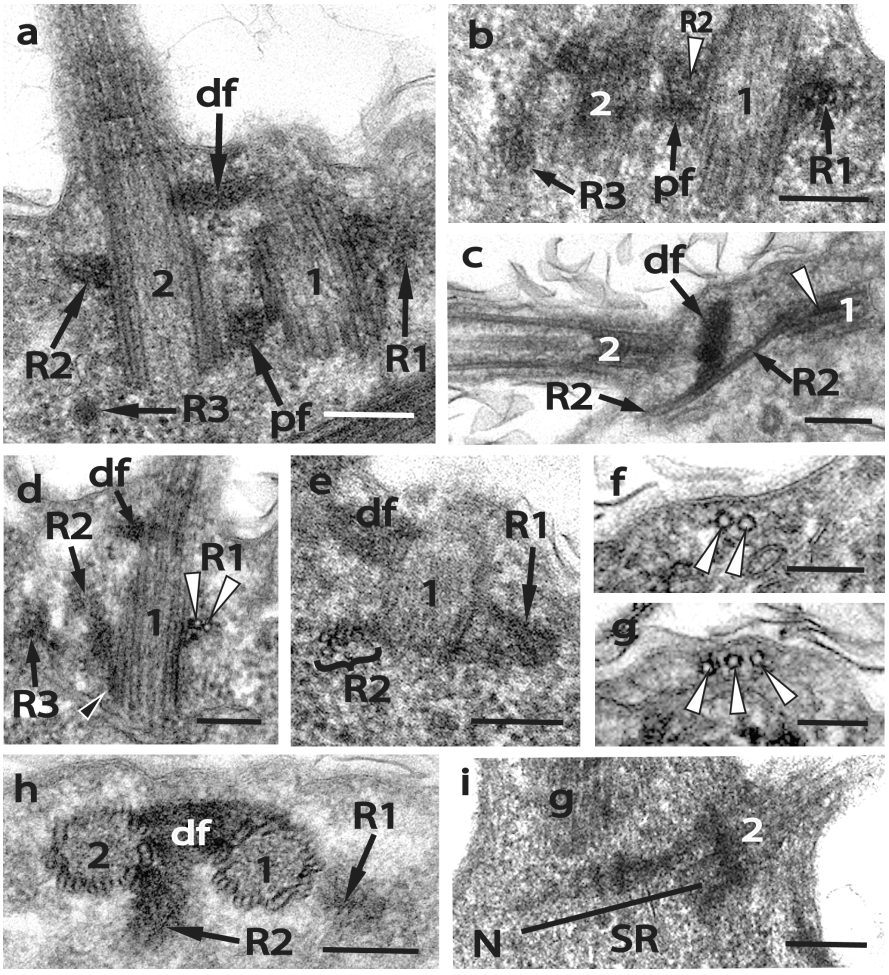

Fig. 8. Thin sections through the flagellar apparatus (FA) of *Microrhizoidea pickettheapsiorum gen. et sp. nov.*. (a) FA viewed from ventro-anterior to dorso-posterior; the immature flagellum and its basal body (2) are on the left while a glancing section of the mature basal body (1) is on the right. The distal fiber (df) connects the distal ends of the basal bodies and the proximal fiber (pf) is located at the proximal ends. A glancing section of the R1 root is visible on the right side of the mature basal body while the R2 root is shown in glancing section emerging from behind the immature basal body. The R3 root is also observed in glancing section. **(b)** Same orientation as in (a), showing the two microtubules of the R1 root in cross-section embedded in dense material at its origin. The R2 root is near its origin just above the proximal fibre (pf) while the R3 root is seen near the base of the immature basal body (2), both in glancing section. **(c)** Section showing the origin of the R2 root. Viewed from left to right, the cell anterior toward the right side of the image. Section is between the two basal bodies (1 and 2) showing the origin of the R2 root along the left side of the mature basal body (white arrowhead). The R2 root passes under the distal fiber (df) toward the surface of the plasma membrane. **(d).** Same orientation as in figures a and b above, showing the mature basal body (1) with a glancing section of the distal fiber (df) and proximal fiber (black arrowhead). The two microtublues of the R1 root (white arrowheads) are observed on the right while the R2 root originates on the left side, just above the proximal fiber. A glancing section of the R3 root is also observed. **(e).** Three or 3+1 microtubules are observed in cross-section at the base of the R2 root near the mature basal body (1) that is seen in glancing section along with the R1 root and the distal fiber (df). **(f)**. Two microtubules (arrowheads) of the R1 root are observed beneath the plasma membrane that has attached body scales. **(g).** Three microtubules of the R3 root are observed beneath the plasma membrane that has attached body scales. **(h).** Cross section of both basal bodies showing the connecting distal fiber (df) and a glancing section of the R2 root which originates on the mature basal body (1) and passes beneath the immature basal body (2). **(i).** A thin, striated root (SR) runs from the base of the immature basal body (2) to the edge of the nuclear envelope and for a short distance down the nuclear surface (N). Note the striations along the line. Scale bars = 25 μm (a-e, h, i), 100 nm (f, g)

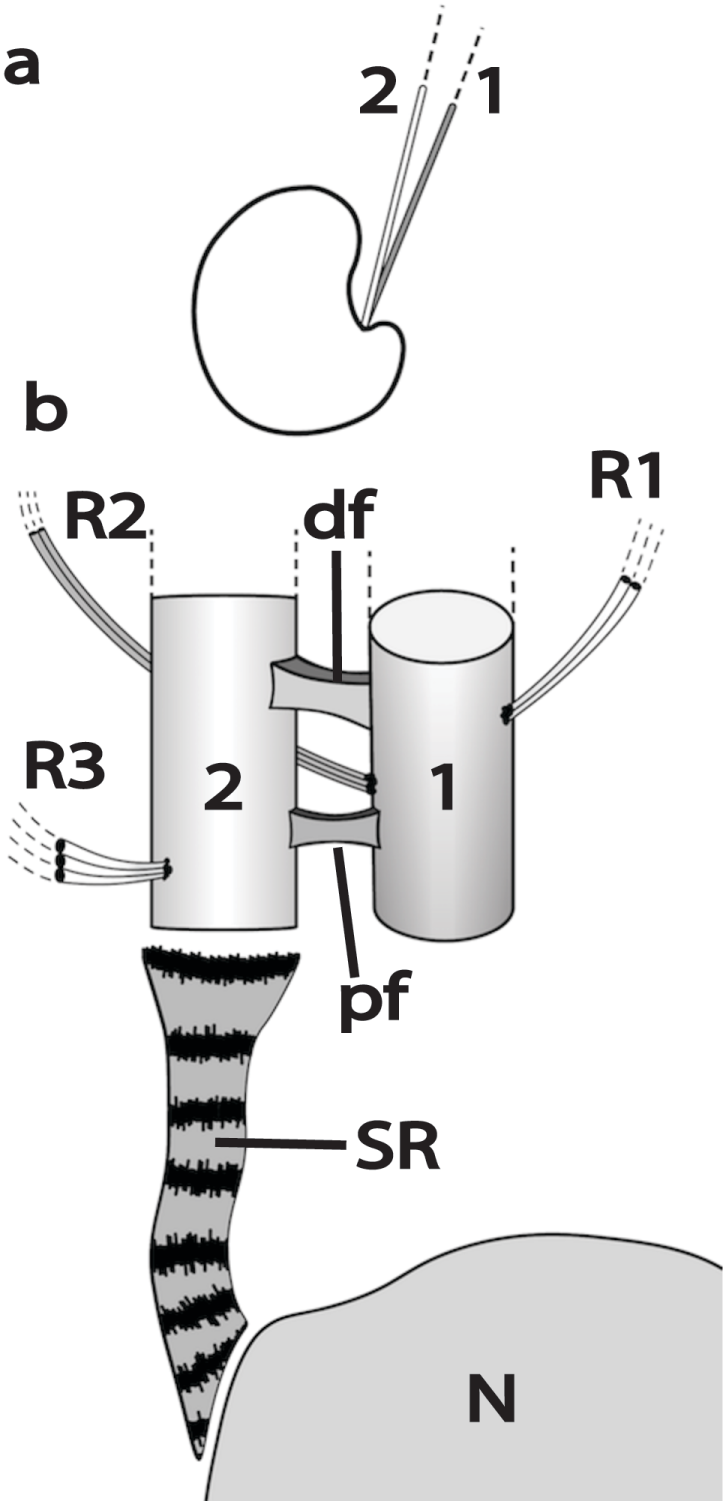

Fig. 9. Diagram of known components of the flagella apparatus of *Microrhizoidea pickettheapsiorum gen. et sp. nov*.. Nucleus (N), microtubular roots R1, R2 and R3, distal fiber (df), proximal fiber (pf), mature basal body (1), immature basal body (2), striated root (SR).

Author/s:
Wetherbee, R; Marcelino, VR; Costa, JF; Grant, B; Crawford, S; Waller, RF; Andersen, RA; Berry, D; McFadden, G; Verbruggen, H

Title:
A new marine prasinophyte genus alternates between a flagellate and a dominant benthic stage with microrhizoids for adhesion

Date:
2019-10-09

Citation:
Wetherbee, R., Marcelino, V. R., Costa, J. F., Grant, B., Crawford, S., Waller, R. F., Andersen, R. A., Berry, D., McFadden, G. & Verbruggen, H. (2019). A new marine prasinophyte genus alternates between a flagellate and a dominant benthic stage with microrhizoids for adhesion. JOURNAL OF PHYCOLOGY, 55 (6), pp.1210-1225. https://doi.org/10.1111/jpy.12909.